Open Archive Toulouse Archive Ouverte (OATAO)

OATAO is an open access repository that collects the work of Toulouse researchers and makes it freely available over the web where possible.

This is a publisher-deposited version published in: http://oatao.univ-toulouse.fr/
Eprints ID: 5362

To link to this article: DOI: 10.1002/cvde.201106888
URL: http://dx.doi.org/doi:10.1002/cvde.201106888

To cite this version: Reuge, Nicolas and Caussat, Brigitte (2011) Modeling of Silicon CVD into Agglomerates of Sub-micrometer-size Particles in a Fluidized Bed. *Chemical Vapor Deposition*, vol. 17 (n° 10-12). pp. 305-311. ISSN 0948-1907

Any correspondence concerning this service should be sent to the repository administrator: staff-oatao@listes-diff.inp-toulouse.fr

Chemical Vapor Deposition

DOI: 10.1002/cvde.201106888

Full Paper

Modeling of Silicon CVD into Agglomerates of Sub-micrometer-size Particles in a Fluidized Bed**

By *Nicolas Reuge* and *Brigitte Caussat**

The aim of the present study is to better understand the mechanisms involved during silicon deposition from silane, SiH_4, into agglomerates of sub-micrometer-size particles treated by fluidized bed (FB)CVD. Two models of silicon deposition into agglomerates assumed either stable, or in permanent formation/desegregation, are developed. In the first case, classical equations of diffusion/reaction in a porous medium are solved, whereas in the second case, the multifluid Eulerian code, MFIX, is used. By comparison with experimental energy dispersive X-ray (EDX) data, modeling results show that the limiting step is not gaseous diffusion into the agglomerates. Very high local deposition rates near the silane entrance probably explain their formation. These results allow us to propose original deposition conditions involving much lower local deposition rates, which should limit agglomeration due to CVD.

Keywords: Agglomeration, Fluidized bed, Modeling, Silane, Silicon

1. Introduction

Modifying the outer surface of sub-micrometer- and nanometer-size particles to improve or modify their useful properties, and then produce innovative materials, is a great challenge.[1,2] Numerous studies[1–10] have proved the efficiency of FBCVD technology in coating powders by various materials, including oxides, metals, and silicon; however a remaining problem when treating micrometer- or nanometer-size powders is related to particle agglomeration and then loss of the initial particle granulometry due to deposition.[2,4,8,9] Indeed such fine particles, belonging to Geldart's group C (cohesive particles), are not suitable for fluidization.[11] They can only be fluidized as agglomerates, of several hundreds of micrometers in diameter, in activated fluidization processes (i.e., mixing with easy-to-fluidize particles, fluidization combined with mechanical stirring, horizontal or vertical vibration). This is due to the strong inter-particle forces (especially Van der Waals forces) existing in beds of such fine particles. Combining CVD and activated fluidization processes tends to transform ephemeral agglomerates of physically bonded particles into definitive agglomerates of chemically bonded particles by the deposition.[2,4,8,9] Of course, this loss of particle granulometry is not acceptable for most industrial applications.

Previous studies in our group[8–10] have been conducted concerning silicon nanodot deposition from the gaseous precursor SiH_4, on micrometer-size TiO_2 particles by mechanically vibrated FBCVD. Optimal vibro-fluidization conditions were first researched in order to minimize the size of agglomerates of physically bonded particles. Subsequently deposition conditions involving very low deposition rates were applied in order to favor reactive diffusion into the particle agglomerates, and then to minimize the formation of definitive agglomerates of TiO_2 particles chemically bonded by silicon. For the experimental conditions tested, however, the particles, on average, were always in the form of agglomerates of several hundreds of micrometers, the biggest agglomerates (of millimeter size) always being formed at the silane entrance near the distributor. A positive result was that the deposition was uniform around each individual TiO_2 particle, probably thanks to the low deposition rates imposed.

The mechanisms of physical agglomeration of sub-micrometer-size particles in fluidized beds, and then of CVD in such agglomerates, are poorly known. In particular, it is difficult to determine if the physical agglomerates formed in the fluidized bed before CVD are dynamic, i.e., constituted of permanently renewed particles, or stable, i.e., always formed of the same particles. In this last case, chemical deposition would then be very close to chemical vapor infiltration (CVI), with a combination of diffusion and reaction mechanisms in a porous medium, whereas in the former case, deposition on quasi-individual particles could be considered.

The aim of the present study is to model silicon deposition into either stable or dynamic agglomerates. First, the experimental results previously obtained by our group

[*] Dr. N. Reuge, Prof. B. Caussat
Laboratoire de Génie Chimique, UMR CNRS 5503, ENSIACET/INPT, University of Toulouse, 4 allée Emile Monso, BP 84234, 31432 Toulouse Cedex 4 (France)
E-mail: Brigitte.Caussat@ensiacet.fr

[**] This work has been supported by the French Midi Pyrénées region council.

 © 2011 WILEY-VCH Verlag GmbH & Co. KGaA, Weinheim

and used for the present modeling study will be detailed. The chemical reactions and kinetic laws employed will then be presented before a description of the models. The modeling results will be compared to the experimental data in order to determine if the agglomerates can be considered as stable or dynamic. These results will also be analyzed to better understand the origin of chemical agglomeration. Finally, original deposition conditions will be proposed, aiming to minimize this agglomeration phenomenon and then preserve the initial particles' micrometer-size granulometry.

2. Previous Experimental Results

In previous experimental works,[8,9] we have studied the vibrated FBCVD process with the aim of depositing nanometer-size layers of silicon from silane around each individual grain. The inlet mass percentage of silane in nitrogen ($<4\%$) and the temperature ($<600\,^{\circ}C$) were chosen in order to work in conditions for which the heterogeneous reaction rate is low in comparison with the gaseous species transport, to limit agglomeration of individual TiO_2 particles due to silicon deposition. 450 g of particles were treated per run, corresponding to a fixed bed-height to column-diameter ratio close to 5. All the tested conditions and the corresponding results are detailed elsewhere.[9] For the present work, we have selected only 2 runs, corresponding to either very high (run A2, 28 g) or very low (run A3, 3.5 g) injected silicon masses, as detailed in Table 1.

Experimental results are detailed in Table 2. The conversion rate of silane deduced from the outlet hydrogen percentage was always close to 100%, thanks to the low inlet percentage of silane used, and to the high specific surface area of powders. The theoretical deposit thickness (assuming uniform Si coating on perfectly spherical particles) was around 5 nm. The corresponding deposition rate was $0.44\,g\,min^{-1}$ for run A2, and logically, lower ($0.05\,g\,min^{-1}$) for run A3.

Whatever the mass of silicon deposited (between 1 g and 28 g), TiO_2 particles after FBCVD were in the form of agglomerates.[10] As observed during pure fluidization (see the Experimental section), the diameter of agglomerates decreased from the distributor zone toward the upper part of the bed. Their mean diameter, measured by sieving, was 330 μm after run A2 and 392 μm after run A3. They were, however, quite friable since, as reported elsewhere,[9] these agglomerates were no longer visible (i.e., exploded) when the diameter distribution of particles after FBCVD was measured by laser granulometry under an air over pressure of 4 bar.

A surprising result was that their mechanical resistance was strong enough to allow the fluidization of the treated particles without any reactor vibration.[10] The minimum fluidization velocity, U_{mf}, was equal to $4.2\,cm\,s^{-1}$ and $3\,cm\,s^{-1}$, respectively, without and with vibrations. The bed expansions were very similar with and without vibration. Visually, without vibration, a bubbling regime was identified just after the minimum of fluidization. Bubbles then grew rapidly with gas velocity. A slugging regime was observed for the highest gas velocities tested ($>10\,cm\,s^{-1}$). The behavior of these powders was then very similar to that of easy-to-fluidize Geldart's group B particles. This result allowed the modeling of the fluidized bed hydrodynamics during CVD experiments, considering the mean diameter of agglomerates without reactor vibration, using the Eulerian code MFIX, as detailed in Section 5.

Some agglomerates obtained after runs A2 and A3 have been slightly crushed, in order to be analyzed in cross-section by scanning electron microscopy (SEM)-EDX. About ten agglomerates per run have been analyzed. Figure 1 presents the average ratios of the mass percentages of silicon and of titanium measured along the agglomerates' radii; for run A3, the measured ratios have been multiplied by ten for a better comparison. After run A2 (26 g of Si deposited), a slight decrease of the Si percentage from the outer part to the centre of the agglomerates can be observed,

Table 1. Experimental deposition conditions.

Run	Temperature gradient before silane injection [°C cm^{-1}]	Mean bed temperature [°C]	Total gas flow rate [L h^{-1} under normal conditions]	Inlet wt.-% of SiH_4	Mass of silicon injected [g]	Deposition duration [min]
A2	2.1	593	669	3.8	28.1	60
A3	1.8	593	642	0.5	3.5	60

Table 2. Experimental results.

Run	Temperature gradient at the end of the runs [°C cm^{-1}]	Vol.-% of H_2	Mass of Si deposited (from the vol.-% of H_2) [g]	Theoretical thickness of deposition [nm]	Deposition rate [g min^{-1}]
A2	1.3	6.37	26.6	8.2	0.44
A3	1.35	0.86	3.45	1.1	0.05

 © 2011 WILEY-VCH Verlag GmbH & Co. KGaA, Weinheim

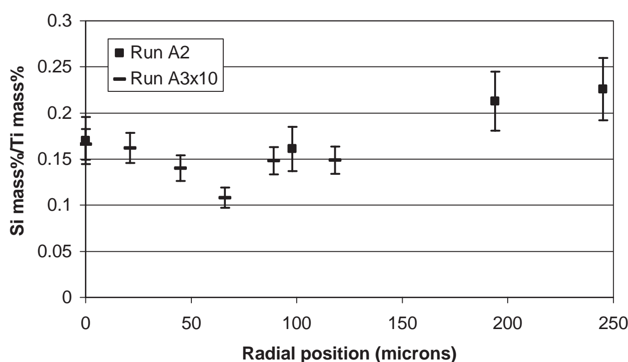

Fig. 1. EDX ratios between silicon and titanium mass percentages along agglomerates' radii after runs A2 and A3 (0 in radial position refers to the center of agglomerates).

whereas the Si percentage remains constant along the agglomerates' radii after run A3 (3.5 g of Si). The result after run A2 can be due to a progressive lowering of the silane concentration towards the centre of the agglomerates during the diffusion/reaction process. This is a frequent issue in CVI. The various possible mechanisms involved have been analyzed by modeling as detailed below, considering the fluidized TiO_2 agglomerates either stable or dynamic.

3. Chemical Reactions and Kinetic Laws

Silane pyrolysis occurs from a temperature of about 350 °C.[5] In a previous work[12] we have performed a detailed analysis of the chemical reactions and kinetic laws available for our FBCVD conditions. The most appropriate kinetic model was shown to be FUR.[12] It has been used here and is briefly recalled below.

Silane first homogeneously decomposes to give the highly reactive chemical species silylene (SiH_2), $SiH_4 \underset{k_{-1}^{hom}}{\overset{k_1^{hom}}{\rightleftarrows}} SiH_2 + H_2$ (R_{hom}). We use the kinetics of Coltrin et al.[13] for the forward reaction, Equation 1.

$$k_1^{hom} = 1.09 \times 10^{25} T^{-3.37} \exp(-256232/R_{PG}T) \quad (1)$$

The backward reaction constant has easily been determined from forward reaction rates and thermochemical properties of the involved species.[14] We have shown[12] that it is useless to consider the subsequent species and homogeneous reactions involved in silane pyrolysis for the low inlet silane concentration studied.

Then silane and silylene can react to form silicon deposition, following the two heterogeneous reactions, $SiH_4 \xrightarrow{k^{het1}} Si_{(s)} + 2H_2$ (R_{het1}), and $SiH_2 \xrightarrow{k^{het2}} Si_{(s)} + H_2$ (R_{het2}).

For (R_{het1}), the Furusawa et al.[15] kinetic law has been shown to be the most appropriate for the FBCVD conditions tested.[12] Since we always used low inlet mass fractions of silane, the Furusawa kinetics can be considered as first order in silane and can then be written as Equation 2.

$$k_1^{het} = 2.15 \times 10^8 \times \exp(-191500/R_{PG}T) \quad (2)$$

For Coltrin et al.[16] and for most authors, all radical species coming from silane pyrolysis have a sticking coefficient of 1. Therefore, the kinetics of silylene SiH_2 deposition is given by Equation 3.

$$k_2^{het} = 13.28\sqrt{T} \quad (3)$$

For kinetic laws, Equations (1) to (3), R_{PG} is equal to 8.314 J mol^{-1} K^{-1}, T is in K, $k_1{}^{hom}$ in s^{-1}, k^{het1} and k^{het2} in m s^{-1}.

4. Deposition Modeling in the Case of Stable Agglomerates

The problem here corresponds to a typical CVI case. The agglomerates have been considered as perfectly spherical and presenting a uniformly distributed porosity. The diffusion/reaction equation of the active species (SiH_4 or SiH_2 diluted in N_2) in an agglomerate is given by Equation 4.

$$-D^{eff}\left(\frac{\partial^2 c}{\partial r^2} + \frac{2}{r}\frac{\partial c}{\partial r}\right) = -R \quad (4)$$

D^{eff} is the effective diffusivity of SiH_4 or SiH_2 in the agglomerate, c the SiH_4 or SiH_2 concentration, r the radial position in the agglomerate and R the consumption rate of silane or silylene by the heterogeneous reactions.

Since the heterogeneous reactions are first order, R (in mol m^{-3} s^{-1}) can be written as Equation 5.

$$R = \sigma_V k^{het} c \quad (5)$$

σ_V is the volumic surface of the porous agglomerate, and k^{het} the kinetic constant. The calculations of σ_V and D^{eff} are detailed as Supplementary Material.The Thiele modulus[17] is given by Equation 6.

$$\phi = \sqrt{\frac{\sigma_V k^{het} r_a^2}{D^{eff}}} \quad (6)$$

r_a is the agglomerate radius. Equation (4) can then be written as Equation 7.

$$\frac{\partial^2 c}{\partial r^2} + \frac{2}{r}\frac{\partial c}{\partial r} = \frac{\phi^2}{r_a} c \quad (7)$$

The boundary condition at the outer surface of the agglomerates is given by Equation 8.

 © 2011 WILEY-VCH Verlag GmbH & Co. KGaA, Weinheim

$$c(r = r_a) = c_s \quad (8)$$

c_s is the active species concentration at the agglomerate outer surface. Equation 7 has an analytical solution given by Equation 9.

$$c(r) = \frac{r_a}{r} \cdot \frac{\sinh\left(\phi \frac{r}{r_a}\right)}{\sinh(\phi)} \cdot c_s \quad (9)$$

The relative difference of reactive concentration between the outer surface and the centre of the agglomerate is then given by Equation 10.

$$\frac{\Delta c}{c} = \frac{c_s - c(r = 0)}{c_s} = 1 - \frac{\phi}{\sinh(\phi)} \quad (10)$$

Table 3 presents the $\Delta c/c$ values obtained for silane and silylene for various agglomerates' radii. First, whatever the agglomerate diameter considered, the $\Delta c/c$ ratio for silylene is always 100%. This means that Si deposition from SiH_2 occurs only on the outer surface of agglomerates. This is not surprising since the sticking coefficient of SiH_2 is equal to 1, which implies that the probability for SiH_2 to diffuse into the agglomerate before chemisorbing is close to zero. Then for silane, it appears that, for agglomerates of diameters equal to or higher than the mean agglomerate diameter (360 μm), the $\Delta c/c$ ratio is close to 100%. This means that silicon is deposited on the agglomerate outer surface and not at its centre. This result is in contradiction to the EDX results. As a consequence, the assumptions that the agglomerates are stable for the conditions tested, or that gaseous diffusion into the agglomerates is the limiting step are not valid; agglomerates can be considered as dynamic.

5. Deposition Modeling in the Case of Dynamic Agglomerates

We now suppose that the agglomerates are perfectly dynamic, i.e., each constitutive particle is either at the centre or at the periphery of the agglomerate. On a sufficiently large time scale, each particle is then coated by the same silicon mass, so we have supposed that the gaseous diffusion is infinitely rapid into the agglomerates and that deposition is then uniform inside them. From a modeling point of view, deposition has been assumed to occur on the total specific surface area of the agglomerates, which means on the surface of each individual TiO_2 grain.

For this part, we used the multifluid Eulerian model of the FBCVD process we had previously developed.[18,19] This model is based on the CFD open-source code MFIX,[20] a benchmark tool for the simulation of gas-solid systems. Calculations were performed using the continuum model, the drag law of Benyahia et al.,[21] and the kinetic theory of granular materials with the differential form of the granular temperature equation for the solid-phase stress tensor in the viscous regime. The solid-phase stress tensor in the plastic regime was treated using the Princeton[22] model. The summary of the governing equations are given in the literature,[21] the expressions of the granular stress model employed in Reuge et al.,[19] and the details can be obtained from MFIX documentation.[21] The chemical reactions and kinetic laws considered are those detailed in Section 3. The bed hydrodynamics have been calculated using the mean diameter of agglomerates as the particle mean diameter, and considering a minimum fluidization velocity of 4.2 $cm\,s^{-1}$ at STP under non-vibrated conditions. The other parameters (grid features, boundary conditions, internal angle of friction, restitution coefficient) are those described in Reuge et al.[12] All results below correspond to steady-state conditions.

Figure 2 shows the calculated evolution of the radially averaged silane mass fraction along the first millimeters of bed height for runs A2 and A3. For run A2, 99% of silane is consumed at 6 mm above the distributor and 84% after 1 mm. For run A3, (with a much lower inlet silane mass fraction than run A2), 99% of silane is consumed after 2 mm.

The corresponding evolution of the radially averaged silicon deposition rate from silane along the bed height is presented in Figure 3. It appears that the deposition rate in the first millimeter near the distributor is very high, more than 90 $nm\,min^{-1}$ for run A2 and 10 $nm\,min^{-1}$ for run A3. These extremely high values of silicon deposition rate near the distributor probably explain the intense agglomeration phenomena in this zone. Moreover, for run A2, the deposition rate is equal to zero after 3 mm above the distributor, and for run A3 after 1 mm. The active zone for deposition is then extremely small. The uniformity of deposition observed by transmission electron microscopy (TEM) around each grain at the end of experiments[8–10] is then due to the intense axial mixing of particles generated by fluidization.

For these two runs, MFIX results have shown that the SiH_2 contribution to deposition is negligible. This can be

Table 3. Calculated relative difference of reactive concentration considering stable agglomerates of various radii r_a.

Reactive species	Δc/c [%] $r_a = 5$ μm	Δc/c [%] $r_a = 50$ μm	Δc/c [%] $r_a = 100$ μm	Δc/c [%] $r_a = 180$ μm	Δc/c [%] $r_a = 250$ μm
SiH_4	0.6	41	82.5	98.5	99.8
SiH_2	100	100	100	100	100

 © 2011 WILEY-VCH Verlag GmbH & Co. KGaA, Weinheim

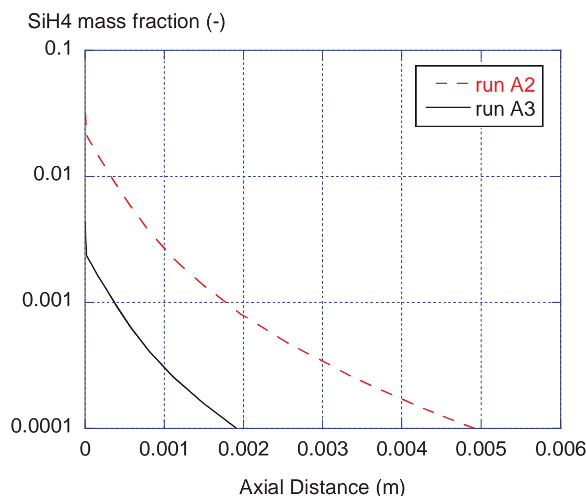

Fig. 2. Evolution of the radially averaged silane mass fraction along the bed height for runs A2 and A3.

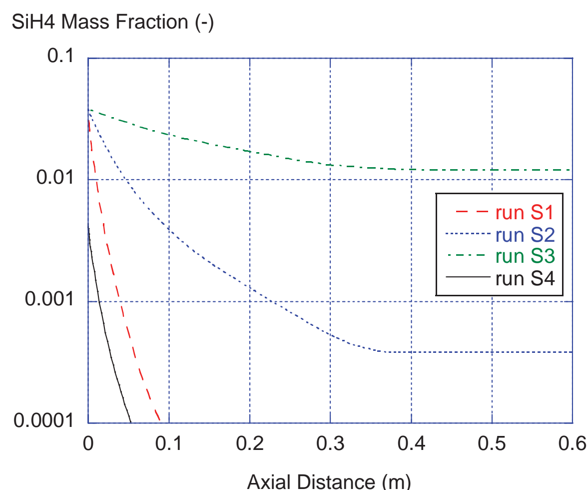

Fig. 4. Evolution of the radially averaged silane mass fraction along the bed height for simulations S1 to S4.

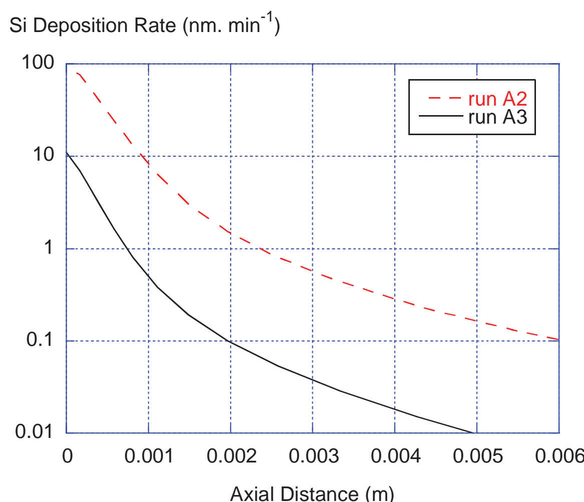

Fig. 3. Evolution of the radially averaged deposition rate from silane along the bed height for runs A2 and A3.

explained by the fact that silane is very rapidly consumed by reaction (R_{het1}). Indeed, the product $k_1^{het}\sigma_V$ is more than 20 000 times higher than the k_1^{hom} constant, so the homogeneous reaction cannot produce any significant amount of silylene.

6. Process Optimization

As previously explained, very high local deposition rates at the silane entrance probably explain particle agglomeration near the distributor, so new MFIX simulations have been performed in order to find conditions leading to a decrease of these local deposition rates to favor reactive diffusion into agglomerates. The most influential CVD parameter is certainly the deposition temperature. As a consequence, four additional simulations have been performed, S1, S2, and S3 with the same inlet mass fraction of silane as run A2, but with bed temperatures equal to 500, 450 and 400 °C, respectively, and S4 with the same inlet mass fraction of silane as run A3 but with a bed temperature of 450 °C. The evolution of the radially averaged silane mass fraction along the bed height for simulations S1 to S4 is presented in Figure 4.

For S1, the silane conversion rate is 99% at 5.6 cm from the distributor, and 23% at the first millimeter; reaction (R_{het1}) is still too rapid. For S2, the silane conversion rate is 99% at the upper level of the expanded fluidized bed (i.e., 34.8 cm), and only of 4% at the first millimeter. Finally, S3 leads to an incomplete conversion rate of silane in the fluidized bed, only equal to 68%, because the bed temperature is too low. These results show that a convenient temperature of deposition for these conditions is 450 °C (S2).

Concerning S4, the silane conversion rate is 99% at only 7 cm above the distributor and not after 34 cm as for S2. This means that the temperature of 450 °C is too high for the low inlet silane mass fraction studied for S4. It logically appears that the inlet mass fraction of silane (ten times lower here than for S2) also acts on the temperature necessary to totally consume silane at a given bed height; the lower the silane mass fraction is, the lower the optimal bed temperature should be.

The corresponding evolution of the radially averaged deposition rate from silane along the bed height for simulations S1 to S4 is presented in Figure 5. The lowering of bed temperature for runs S1 to S3 in comparison with run A2 leads to a high decrease of silicon deposition rates. The maximum deposition rates are, logically, always observed at the silane inlet, and are close to 10, 1 and 0.1 nm min^{-1} for bed temperatures of 500, 450, and 400 °C, respectively. The agglomeration near the distributor should then be lowered

 © 2011 WILEY-VCH Verlag GmbH & Co. KGaA, Weinheim

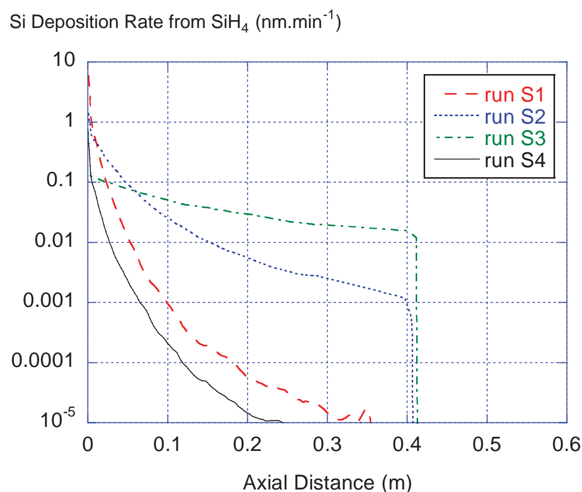

Fig. 5. Evolution of the radially averaged deposition rate from silane along the bed height for simulations S1 to S4.

for these conditions of work. The slope of the deposition rate axial evolution increases with bed temperature because of the higher silane conversion.

According to results in Figure 4, the most interesting conditions are those of run S2. We can observe in Figure 5 that, for this run, the deposition rate decreases from 1 to 0.05 nm min^{-1} on the first ten centimeters of the bed (corresponding to silane mass fraction higher than 0.005) and then decreases to 10^{-3} nm min^{-1} for the upper part of the bed. The first ten centimeters of the bed are active for deposition (to be compared to a few millimeters for run A2). A larger zone of deposition at a much lower deposition rate should minimize particle agglomeration and favor Si deposition uniformity on the whole particle surface.

For run S4, the initial deposition rate is lower than that of run S2 because the silane inlet mass fraction is lower. It is higher than that of run S3 because the temperature of S4 is higher. The slope of its axial evolution is highest because of the very low silane inlet mass fraction. These results confirm the fact that, for run S4, only the first centimeters of the bed are active for deposition.

Finally, for S1 to S4, MFIX results have shown that the silylene contribution to deposition is always negligible because either silane is too rapidly consumed by (R_{het1}) for runs S1 and S4, or the temperature is too low to allow the homogeneous formation of silylene to occur.

7. Conclusion

Previous experimental studies of silicon FBCVD on micrometer-size TiO_2 particles[8–10] have shown that after deposition, particles were in the form of agglomerates of several hundreds of micrometers in mean diameter, the biggest agglomerates always being found near the silane entrance. Most of these agglomerates were friable and TEM and EDX analyses revealed that silicon was deposited quite uniformly around each individual TiO_2 particle.

It is to better understand the mechanisms of deposition into these agglomerates and then to limit agglomeration due to deposition that the present study has been performed.

Two models of silicon CVD from silane into agglomerates of micrometer-size TiO_2 particles have been developed, assuming the agglomerates are either stable, i.e., always formed of the same particles, or dynamic, i.e., constituted of permanently renewed particles. In the first case, classic equations of diffusion/reaction employed in CVI have been solved whereas in the second case, the multifluid Eulerian code MFIX has been used. The comparison of experimental EDX silicon percentage profiles along agglomerates' radii with modeling results has shown that, for the conditions tested, gaseous diffusion into the agglomerates is not a limiting step.

By considering the entire surface of particles available for deposition, MFIX results have then shown that, for the experimental conditions tested, the deposition zone does not exceed a few millimeters near the silane entrance, and that the local deposition rate in this zone can reach 90 nm min^{-1}. Such extremely high values can probably explain the intense agglomeration phenomena experimentally observed in this zone. On the basis of these results, optimized deposition conditions leading to much smaller local deposition rates and larger zones of deposition have been found, which should limit powder agglomeration due to CVD. They typically correspond to temperatures as low as 450 °C for an inlet gas mixture of a few percents of silane diluted in nitrogen. The experimental validation of these original deposition conditions is now in progress.

Such an approach, combining experimental and modeling analyses, is of interest for all researchers working on gas-phase deposition processes on micrometer- and nanometer-size objects forming agglomerates (micro- or nano fibers, nanotubes, nanowires, micro- and nanoparticles).

8. Experimental

As detailed elsewhere [8,9] the FBCVD reactor was made of a vertical cylindrical column of stainless steel with an internal diameter of 0.052 m and a height of 0.8 m. It was externally heated by a three-zone electrical furnace, and the wall temperatures were monitored by three thermocouples. Several thermocouples were also placed into a vertical tube of 6 mm in diameter inside the reactor. An Inconel™ porous plate was used for the gas distribution. Electronic grade silane and N50 nitrogen (Air Liquide) were supplied to the bottom of the bed through ball rotameters connected to manometers. The hydrogen percentage of the exit gas resulting from silicon deposition was measured by a catharometer. A DasyLab® system enabled the on-line acquisition of the differential pressure, hydrogen percentage, and FB temperatures.

The powder used in this study was non-porous TiO_2 particles belonging to the anatase crystalline phase (Sigma Aldrich). Its mean volume diameter was 1.6 µm and its Sauter diameter was 0.7 µm, as measured by laser granulometry. The Sauter diameter must be considered when surface phenomena such as heterogeneous chemical reactions exist. Its grain density was measured by helium pycnometry as equal to 3800 kg m^{-3}; its specific surface area was 10 m^2 g^{-1}, as measured by BET. Its Hausner ratio was 1.86, classifying it into the Geldart's group C [11] i.e., cohesive particles. As a consequence, their fluidization without vibration was impossible; some gas

 © 2011 WILEY-VCH Verlag GmbH & Co. KGaA, Weinheim

channels or fixed paths appeared through the bed, which remained quasi-immobile for the whole range of velocities tested. Vibration was then mandatory to overcome the important inter-particular forces existing in the bed. After a long study [10], some convenient fluidization conditions were found, in particular in terms of frequency and amplitude of vibrations. As it is well-known in the literature for such particles, however, the fluidization of individual TiO_2 grains was impossible. Cadoret [10] has experimentally determined, by numerical image analysis in a vibrated glass column of dimensions identical to that of the FBCVD reactor, that only agglomerates of several hundreds of micrometers in average diameter were fluidized. The agglomerate diameter decreased from the distributor region (where they were millimeter-size) towards the upper part of the bed. It was not possible to determine whether these agglomerates of physically bonded particles were stable (i.e., formed of static particles) or dynamic (i.e., in permanent formation/desegregation).

Received: October 20, 2010
Revised: February 7, 2011

[1] Y. Chen, J. Yang, A. Mujumdar, R. Dave, *Powder Technol.* **2009**, *189*, 466.

[2] J. R. Scheffe, A. Frances, D. M. King, X. Liang, B. A. Branch, A. S. Cavanagh, S. M. George, A. W. Weimer, *Thin Solid Films* **2009**, *517*, 1874.

[3] R. Nauman d'Alnoncourt, M. Becker, J. Sekulic, R. A. Fisher, M. Muhler, *Surf. Coatings Technol.* **2007**, *201*, 9035.

[4] S. Morooka, K. Kusakabe, A. Kobata, *Fluidization VI, Proc. Int. Conf. Fluidization* (Eds: J. R. Grace, L. W. Shemilt, M. A. Bergounou) A.I.Ch.E. **1989.**

[5] T. Kojima, O. Morisawa, *Proc. 8th Eur. Conf. on CVD,* J. Phys. IV France **1991**, 02, C2-475.

[6] B. Caussat, M. Hemati, J. P. Couderc, *Chem. Eng. Sci.* **1995**, *50*(22), 3615.

[7] M. P. Tejero-Ezpeleta, S. Buchholz, L. Mleczko, *Can. J. Chem. Eng.* **2004**, *82*(3), 520.

[8] L. Cadoret, N. Reuge, M. Syamlal, S. Pannala, C. Coufort, B. Caussat, *Powder Technol.* **2009**, *190*, 185.

[9] L. Cadoret, C. Rossignol, J. Dexpert-Ghys, B. Caussat, *Mater. Sci. Eng. B* **2010**, *170*, 41.

[10] L. Cadoret, *Ph. D. Thesis*, INPT, France **2007.**

[11] D. Geldart, *Powder Technol.* **1973**, *7*, 285.

[12] N. Reuge, L. Cadoret, B. Caussat, *Chem. Eng. J.* **2009**, *148*, 506.

[13] M. E. Coltrin, R. J. Kee, G. H. Evans, *J. Electrochem. Soc.* **1989**, *136*, 819.

[14] C. R. Kleijn, *Thin Solid Films* **2000**, *365*, 294.

[15] T. Furusawa, T. Kojima, H. Hiroha, *Chem. Eng. Sci.* **1988**, *43*, 2037.

[16] M. E. Coltrin, R. J. Kee, J. A. Miller, *J. Electrochem. Soc.* **1986**, *133*, 1206.

[17] E. W. Thiele, *Ind. Eng. Chem.* **1939**, *31*, 916.

[18] L. Cadoret, N. Reuge, S. Pannala, M. Syamlal, C. Coufort, B. Caussat, *Surf. Coat. Technol.* **2007**, *201*, 8919.

[19] N. Reuge, L. Cadoret, C. Coufort, S. Pannala, M. Syamlal, B. Caussat, *Chem. Eng. Sci.* **2008**, *63*, 5540.

[20] www.mfix.org.

[21] S. Benyahia, M. Syamlal, T. J. O'Brien, *Summary of MFIX Equations* 2005-4. From URL http://www.mfix.org/documentation/MfixEquations2005-4-1.pdf **2006.**

[22] A. Srivastava, S. Sundaresan, *Powder Technol.* **2003**, *129*, 72.

[23] R. B. Bird, W. E. Stewart, E. E. Lightfoot, *Transport Phenomena*, Wiley International Edition, New York **1960.**

[24] T. C. Zhang, P. L. Bishop, *Water Res.* **1994**, *28*, 2279.

[25] R. P. Dias, C. S. Fernandes, M. Mota, J. A. Teixeira, A. Yelshin, *Int. J. Heat Mass Transfer* **2007**, *50*, 1295.

[26] M. Mota, J. A. Teixeira, R. Dias, A. Yelshin, *Proc. 9th World Filtration Congress*, American Filtration & Separation Society, Richfield, MN USA Paper 316-3 **2004.**

[27] C. N. Satterfield, *Mass Transfer in Heterogeneous Catalysis*, Technical Report MA-41, MIT Press, Cambridge **1970.**

 © 2011 WILEY-VCH Verlag GmbH & Co. KGaA, Weinheim